Physics – Uspekhi **62** (7) 649 – 659 (2019)

REVIEWS OF TOPICAL PROBLEMS PACS numbers: 05.60.Cd, 66.10.C –

Nonclassical transport in highly heterogeneous and sharply contrasting media

L A Bolshov, P S Kondratenko, L V Matveev

DOI: https://doi.org/10.3367/UFNe.2018.08.038423

Contents

Abstract. We review the physical models of nonclassical transport processes in highly heterogeneous media with different types of the spatial distribution of characteristics. We discuss transport in regularly heterogeneous, fractal, and statistically homogeneous sharply contrasting media, as well as in liquid media under the condition of Rayleigh – Benard convection. The behavior of the impurity concentration in the main localization region and at asymptotically large distances from the source is analyzed. The effect on the transport regimes arising due to the presence of colloids, as well as barriers surrounding the impurity source, is investigated. An asymptotic approach to the calculation of the concentration in a medium with large-scale heterogeneities in the distribution of transport characteristics is presented.

Keywords: superdiffusion, subdiffusion, concentration asymptotic form, percolation media, double porosity, sorption

L A Bolshov (*), **P S Kondratenko** (†), **L V Matveev** (‡)
Nuclear Safety Institute, Russian Academy of Sciences,
ul. Bol'shaya Tul'skaya 52, 115191 Moscow, Russian Federation;
Moscow Institute of Physics and Technology
(National Research University),
Institutskii per. 9, 141701 Dolgoprudnyi, Moscow region,
Russian Federation
E-mail: (*) bolshov@ibrae.ac.ru, (†) kondrat@ibrae.ac.ru,
(‡) matweev@ibrae.ac.ru

Received 10 May 2018, revised 13 August 2018
Uspekhi Fizicheskikh Nauk **189** (7) 691 – 702 (2019)
DOI: https://doi.org/10.3367/UFNr.2018.08.038423
Translated by S D Danilov; edited by A M Semikhatov

1. Introduction

Tracer transport is commonly referred to as nonclassical (or anomalous) if the size of the tracer localization domain grows with time according to a power law with an exponent $\gamma \neq 1/2$,

$$R \propto t^{\gamma}, \tag{1}$$

deviating from the square-root law of classical diffusion. The case $\gamma > 1/2$ is referred to as superdiffusion, and the case $\gamma < 1/2$, as subdiffusion. Anomalous transport is encountered in very different branches of the natural sciences, such as plasma physics [1, 2], the physics of semiconductors [3, 4], astrophysics [5], biophysics [6, 7], hydrogeology [8, 9], and many others [10]. A special place in this field is occupied by geological applications, in particular, those related to the practical problem of radioactive waste disposal. An extensive set of field observations has been accumulated over recent years, indicating that in many cases the transport of tracers dissolved in ground waters of geological media cannot be described by the classical theory based on Darcy's and Fick's laws, with deviations possibly reaching several orders of magnitude [11]. This set of problems is the subject of research covered in this review, although the models developed have a much wider range of applicability.

Historically, the first models describing nonclassical transport date back to the 1930s. The first study was apparently that by Khintchine and Levy [12], who treated particle walk as occurring via successive hops of various lengths and durations. If the probability distribution functions for these hops decayed sufficiently slowly with the

length and duration, the resulting mean square displacement of the particle increased with time according to an anomalous law.

Subsequently, this approach was actively used in other models of nonclassical transport, for example, the continuous-time random walk (CTRW) model. This model is based on an averaged description of the migration of a particle ensemble based on the distribution function mentioned above. It is assumed that the medium properties (the probability of hops) are uniform in space. The form of the distribution function has to be derived for concrete physical mechanisms governing the migration of individual particles. Such a model was proposed in [13] and used afterwards to solve numerous anomalous transport problems in very different variants (see, e.g., review [14] and the references therein). We mention recent work [15], which applies this approach to pollution migration in fractured rocks.

Models of 'fractional diffusion' are in fact based on the same principles (they rely on a probability distribution of hops) [16–22]. In CTRW models, the distribution of concentration is derived by summing probabilities of individual hops, but in models of 'fractional diffusion' conservation-law equations are derived to describe the evolution of concentration; however, they contain fractional-order derivatives in time and space. Augmented with boundary conditions, this formulation allows transport problems to be treated in domains composed of subdomains with different properties, and also accounts for the presence of external fields. We emphasize that in CTRW models, as well as in models described by equations with fractional derivatives, the concentration decays as a power law at asymptotically large distances if the tracer transport in the main cloud occurs in an anomalous superdiffusive regime. Applications of these approaches to the analysis of specific physical phenomena can be found in Ref. [10] (see also Refs [23–28]).

An approach to the description of nonclassical transport has been actively developed in recent years, with the system dynamics (the probability and characteristics of hops) possibly dependent on the tracer concentration [29]. In this case, the Fokker–Planck equation is considered as a master equation; its solution can also lead to anomalous transport regimes. In a more general case, models of this type take interactions between tracer particles, including their possible annihilation, into account [30]. The plausibility of this approach can be substantiated if the concentration of migrating particles is sufficiently large.

A number of papers (see, e.g., Ref. [31]) develop an approach where correlations in realizations of successive hops of migrating particles (or more generally, correlations in particle motion [32, 33]) are taken into account. In this case, the nonclassical character of transport is the result of non-Markovian dynamics.

We note that a description of transport based on elementary hops of migrating particles in heterogeneous media is in a certain sense an abstract mathematical tool. In such an approach, it is assumed that the probability distribution functions already incorporate information on the properties of correlations in the distribution of these heterogeneities when the length of an individual hop considerably exceeds the characteristic size of medium heterogeneity. However, when the size of heterogeneities is much larger than the physical mean free path of particles, it seems more natural to base the modeling on specific physical transport mechanisms (advection and diffusion), by taking significant spatial variations in transport constants and actual medium geometry into account. Just such an approach underlies the research leading to the results reviewed here.

The first such approach to the description of nonclassical transport was apparently realized in Ref. [1], where a layered medium was considered with the tracer advected at a constant speed along each layer but with the velocity direction varying randomly from layer to layer. The exchange between the layers was due to diffusion. The resulting mean transport along the layers proved to be a superdiffusive type at times when the tracer cloud occupies many layers. Namely, the growth of the tracer cloud followed the law

$$R \propto t^{3/4} . \tag{2}$$

It is noteworthy that this process was used in Ref. [1] to describe particle transport in a magnetized plasma. Later (after approximately 10 years), it was 'rediscovered' for problems of transport in geological formations [34].

A special feature of transport in geological media is that it occurs as the transport of solute carried by ground waters along channels formed by voids in rock (pores or cracks). The transport mechanisms are advection, i.e., transport with the speed of local flow, and molecular diffusion in the solution. As a result, an equation for the concentration in channels takes the form of the mass conservation law with a classical flux, including advection and diffusion.

To advance the theory further, it is necessary to average the equation for concentration over an ensemble of realizations. Two factors are of key importance here: the channel geometry and strong contrast in the distribution of medium properties.

As concerns the first factor, all media can be divided into three classes depending on correlations in the distribution of heterogeneities: (1) the simplest class comprises regularly heterogeneous media, for example, a crack in a porous medium; (2) statistically homogeneous and sharply contrasting media; (3) percolation media or media having fractal properties within some large spatial scale.

The essence of the second factor lies in the following. If we have a fractured, porous (for example, geological) medium with sufficiently long cracks, a fluid percolates through the cracks much more efficiently than through the surrounding porous matrix. The difference is typically so large that in the first approximation we can disregard filtration through the porous matrix and consider only diffusion. It can be assumed that the medium consists of two subsystems of high and low permeability. Such an approximation bears the name of the dual-porosity medium. Examples of such media are furnished by isolated cracks in a porous matrix, fractured porous media with a continuous distribution of cracks, or sand–clay formations.

This review is structured as follows. In Sections 2–4, we consider nonclassical transport in regularly heterogeneous, percolation and statistically homogeneous media. In Section 5, we analyze the effect of sorption on transport. Transport processes in periodic flows caused by Rayleigh–Benard convection are considered in Section 6. In Section 7, we discuss the role of a weakly permeable protective barrier bounding a tracer source. In Section 8, we present an asymptotic approach to computations of concentration for transport in a medium with large-scale heterogeneities. Brief conclusions are formulated in Section 9.

2. Regularly heterogeneous media

2.1 Problem statement

We consider transport in a regularly heterogeneous medium in the following geometry. The medium consist of two domains: a geometrically regular, strongly permeable domain I, referred to as a crack for convenience, and the remaining space (domain II) filled with a porous matrix of low permeability. Furthermore, we consider cracks shaped like a planar layer of thickness a (Fig. 1a) and an infinite cylinder of cross-sectional area $s \sim a^2$ (Fig. 1b).

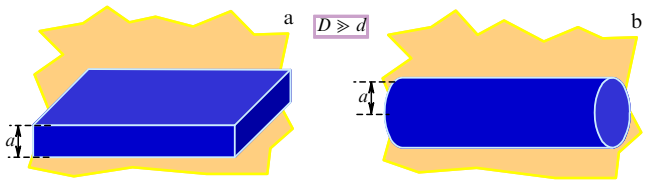

Figure 1. Regularly heterogeneous media.

We first assume that the transport in both domains is determined by diffusion, and therefore the concentration $n(\mathbf{r}, t)$ in domain I satisfies the equation

$$\frac{\partial n}{\partial t} = D\Delta n\,, \tag{3}$$

and the concentration $c(\mathbf{r}, t)$ in domain II satisfies the equation

$$\frac{\partial c}{\partial t} = d\Delta c\,. \tag{4}$$

A sharp contrast in properties implies that a strong inequality holds,

$$D \gg d\,. \tag{5}$$

Concentrations and normal components of fluxes are equal at the boundary between the domains. Initially, the tracer is entirely localized in the crack at the coordinate origin. This model was first proposed by Dykhne [36], and we therefore call it the Dykhne model.

2.2 Tracer behavior in the main localization domain

A qualitative analysis shows that the character of transport in such a system depends on the time interval. At small times $t \ll t_1$, where

$$t_1 = \frac{a^2}{4d}\,, \tag{6}$$

the fraction of tracer leaving the crack is negligibly small and transport along the crack follows the classical diffusion law with the coefficient D. For $t > t_1$, particles walking randomly leave the crack temporarily, and as t increases, they spend progressively less and less time in the crack and for $t \gg t_1$ mainly stay in the matrix. In this case, during a certain time interval, just as for $t < t_1$, the transport is governed by diffusion in the crack. The fraction of time particles spend in a planar crack and hence diffuse in the plane of the crack with the coefficient D, can be estimated as $\tau(t) \sim a/\sqrt{dt}$. Therefore, the size of the tracer cloud containing the main portion of the tracer grows in the plane of the crack in accordance with the law

$$R^2(t) \sim \int_{t_1}^{t} D\tau(t')\,\mathrm{d}t' \sim D\sqrt{t_1 t}\,. \tag{7}$$

Transport in the matrix along the crack makes very small contribution at this stage and thus the matrix acts as a trap. This is the reason for the anomalous, subdiffusive regime $R \propto t^{1/4}$.

In essence, according to Eqn (7), the tracer is transported with the effective (time-dependent) diffusion coefficient, equally weighted over the domains occupied by the tracer, including both the fast and slow subdomains. The validity of this reasoning relies on the transport in both subsystems being concerted owing to the conditions on the boundary between them.

Similarly, for the fast medium shaped as an infinite cylinder, the size of the tracer cloud along the cylinder axis grows as

$$R(t) \sim \sqrt{Dt_1 \ln \frac{t}{t_1}}\,, \tag{8}$$

where $t_1 = s/(4d)$.

Such (subdiffusive) regimes of transport take place for the current time $t_1 \ll t \ll t_2$, where

$$t_2 = \left(\frac{D}{d}\right)^2 t_1 \tag{9}$$

for a planar layer and

$$t_2 = t_1 \frac{D}{d} \ln \frac{D}{d} \tag{10}$$

for a cylinder. For times $t \gg t_2$, the fraction of time particles spend in the crack is so small that it no longer influences the transport, which is now determined by the properties of the matrix. As a result, for $t \gg t_2$ the transport regime corresponds to slow classical diffusion with a small coefficient d. Thus, the Dykhne model exhibits fast classical diffusion at times $t \ll t_1$, subdiffusion in the interval $t_1 \ll t \ll t_2$, and slow classical diffusion at times $t \gg t_2$.

Similarly, a generalized Dykhne model was considered, which adds advection with a constant velocity $\mathbf{u}$ in the crack to the diffusion (the vector $\mathbf{u}$ either lies in the plane of the crack or is directed along the cylinder axis) [37]. In this case, the system behavior depends on the Peclet number $\mathrm{Pe} = ua/d$ characterizing the relative importance of advection and diffusion. For $\mathrm{Pe} \ll 1$, the tracer behavior is described by the same laws as in the original Dykhne model. For $\mathrm{Pe} \gg 1$, new nonclassical, quasidiffusive regimes take place [38]. In these regimes, the mean particle displacement $X(t)$ increases with time by the same law as the tracer cloud size $R(t)$. The front propagation speed depends on the crack shape. For a planar crack, the front displacement is proportional to the square root of time,

$$X(t) \sim R(t) \sim \sqrt{D_u t}\,, \tag{11}$$

where

$$D_u = u^2 t_1 \tag{12}$$

is the so-called quasidiffusion coefficient. For an infinite cylinder, quasidiffusion is logarithmic,

$$X(t) \sim R(t) \sim ut_1 \ln \frac{t}{t_1}\,. \tag{13}$$

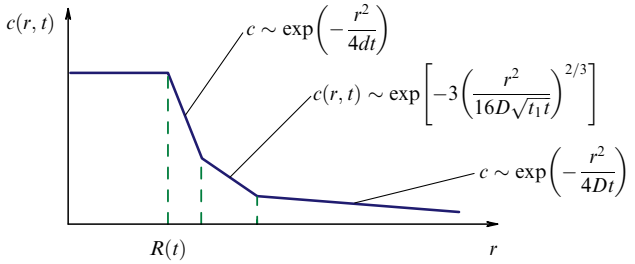

Figure 2. Many-stage structure of concentration at asymptotically long distances from the source for $t \gg t_2$ for a crack in the form of a planar layer.

2.3 Asymptotic behavior of concentration at large distances

All the regimes listed in Section 2.2, obtained previously from qualitative estimates [39, 40], can be derived from the exact problem solution. The exact solution also enables computations of concentration behavior at asymptotically large distances from the source, $r \gg R(t)$. This behavior also depends on the time interval. At small times, the concentration decays as a Gaussian curve and is characterized by a large diffusion coefficient. When the regime in the main part of the cloud is superseded by a subdiffusive one, the asymptotic behavior becomes two-stage. The closer stage is described by a stretched exponential and corresponds to subdiffusion, and the further stage by a Gaussian exponential with a large diffusion coefficient (as in the regime over the preceding time interval). At the latest times, the asymptotic behavior becomes three-stage: its two distant parts are the previous ones, and the closest part is determined by the current regime of slow classical diffusion.

Such a structure of asymptotic behavior at large times for a planar crack is shown schematically in Fig. 2.

Thus, the following conclusions can be drawn from the Dykhne model: in media with sharp property contrast, low-permeability domains serve as traps that considerably slow the tracer transport. This slowdown leads to the occurrence of subdiffusive regimes that depend on the medium geometry and transport mechanisms. The change of transport regimes in the main cloud leads to an asymptotic behavior for the concentration that combines several stages. The following law is observed: more distant parts of the asymptotics are governed by earlier transport regimes in the main cloud. The closest stage corresponds to the current regime.

3. Percolation media

We turn to media in which the system of high-permeability channels has the form of a percolation cluster [41, 42]. In nature, this situation is encountered in fractured geological formations [43] and in porous media characterized by a large spread of pores over sizes. A specific feature of percolation media is that in the range of large spatial scales, starting with a certain scale denoted by a and up to the correlation radius ξ, they are fractal and have the property of scale invariance. At scales larger than ξ, these media become statistically homogeneous.

We note that percolation clusters have their own internal structure [41]: they consist of a backbone permeating all the structure and facilitating transport over long distances, and traps, which are of finite size, being connected to the backbone at a single point. An example of a percolation cluster in the framework of the random connection model is given in Fig. 3.

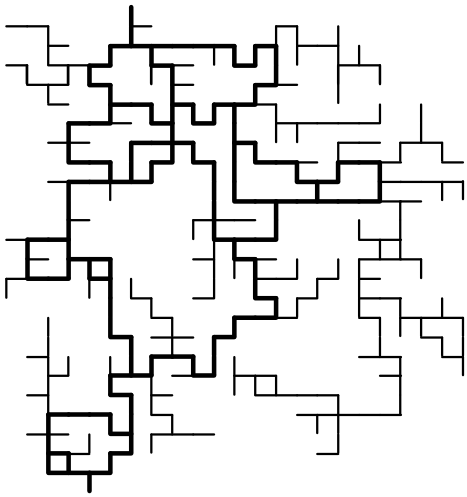

Figure 3. Diagram of a percolation cluster. The main trunk is marked by a thick line, traps are shown by thin lines.

3.1 Isotropic model of random advection with long-range correlations

In an isotropic model of random advection with long-range correlations, only advection in the backbone is accounted for as a transport mechanism in a percolation medium. The tracer escaping to the traps and matrix is ignored.

The equation for the microscopic concentration $\hat{c}$ for transport in a percolation cluster takes the form of the standard conservation law with the flux determined by advection in a random velocity field:

$$\frac{\partial \hat{c}}{\partial t} + \operatorname{div}(\mathbf{V}\hat{c}) = 0\,. \tag{14}$$

The theory aims to describe transport for quantities averaged over an ensemble of realizations, $c = \langle \hat{c} \rangle$. The velocity field is taken as incompressible. The correlation length ξ in the velocity distribution is set to infinity. The ensemble mean velocity is assumed to be zero, and hence the velocity correlation functions become the characteristics determining transport.

As we have already noted, at scales $r \gg a$, the medium has fractal properties (a carries the name of the lower fractal bound). Therefore, there is no spatial scale characterizing the system in this range, which in turn allows using ideas from the theory of critical phenomena [44, 45], assuming that at scales $r \gg a$ the transport process has a property of scale invariance. This implies that under a similarity transformation $\mathbf{r} \to \lambda\mathbf{r}$, an arbitrary quantity changes as $A \to \lambda^{\Delta_A} A$. The exponent Δ_A carries the name of the scaling dimension of A. The velocity pair correlation function for $|\mathbf{r}_1 - \mathbf{r}_2| \gg a$ then takes the form

$$\left\langle \mathbf{V}(\mathbf{r}_1)\mathbf{V}(\mathbf{r}_2) \right\rangle \propto V^2 \left(\frac{a}{|\mathbf{r}_1 - \mathbf{r}_2|} \right)^{2h}, \tag{15}$$

where h is the scaling dimension of velocity. We suppose that an n-point correlation function of advective velocity acquires the factor λ^{nh} under the coordinate transformation $\mathbf{r} \to \lambda\mathbf{r}$, in analogy with pair correlator (15).

Turning to the description of concentration averaged over an ensemble of realizations, we start with Eqn (14) and in the general case obtain an integro-differential equation that has been studied by different techniques: based on the analysis of scaling dimensions [46] and with the help of Feynman diagrams [47]. Both methods lead to identical results consisting of the following. The character of tracer transport depends on the character of correlation function decay, i.e., on the parameter h. If $h > 1$, transport occurs in the classical diffusion regime, and hence the concentration is described by a Gaussian profile, also at asymptotically large distances. For $h < 1$, a superdiffusion regime is realized, and the size of the tracer cloud grows with time as

$$R(t) \sim (a^h V t)^{\gamma}, \qquad \gamma = \frac{1}{1+h}. \tag{16}$$

It is worth noting that the concentration decay is asymptotically described by a 'compressed' exponential,

$$c(r,t) \cong \frac{B}{(4\pi)^{3/2} R^3(t)} \left(\frac{r}{R(t)}\right)^{3(2\gamma-1)} \times \exp\left[-\left(C\,\frac{r}{R(t)}\right)^{1/(1-\gamma)}\right], \tag{17}$$

where $R(t)$ is given by formula (16), and B and C are constants of the order of unity. Thus, the decay at long distances becomes faster than in the classical case [46].

We stress that the problem statement analyzed here, as well as other problems with tracer transport, assumes fixed initial conditions for the concentration distribution.

The medium considered in this section is fractal but also spatially disordered. The resultant concentration is the mean over an ensemble of medium realizations, in the same sense as for correlation functions of the advecting velocity. Estimates made under the assumption of an infinite correlation radius indicate that in the statistical description of transport processes the uncertainty of relative concentration in the model of random advection can reach the order of unity.

Furthermore, to accommodate the random advection model for real media, we consider the influence of the following factors: the finiteness of the correlation length, the anisotropy of percolation media, and the role of traps (dead ends and the low-permeability matrix surrounding a percolation cluster).

We note that the model of random advection was explored previously in Refs [48, 49], where relations for the main domain of tracer localization were obtained. However, the question of the concentration asymptotics was left open.

3.2 Percolation media with a finite correlation length

If the correlation length is finite, $\xi < \infty$, the tracer behavior depends on the time interval [50]. Over the time intervals such that the tracer cloud size is less than the correlation radius ξ, the properties of the medium that govern the transport remain the same as in an infinite fractal medium. Therefore, under the condition $h < 1$, transport occurs in a superdiffusive regime according to law (16). In time intervals such that the cloud size exceeds ξ, $t \gg t_\xi$, the medium becomes statistically homogeneous and hence transport occurs in the classical diffusive regime. We note that on a qualitative level, this result was obtained in numerical simulations of particle diffusion over a fractal cluster with a finite correlation length in Ref. [51], where at large times the transition from subdiffusion to classical diffusion was observed.

The effective diffusion coefficient is defined by the relations

$$D_{\text{eff}} \sim \frac{\xi^2}{t_\xi}, \qquad t_\xi \sim \frac{\xi^{1+h}}{V a^h}. \tag{18}$$

The laws of concentration behavior at asymptotically large distances are as follows. At times smaller than t_ξ, the concentration decay with an increase in distance is described by a compressed exponential, as previously. At large times $t \gg t_\xi$, the asymptotic behavior becomes two-stage. The closer stage corresponds to the current regime of classical diffusion, and the further stage corresponds to the preceding regime of superdiffusion. The asymptotic structure here obeys the general rule established for regularly heterogeneous media: the further the stage, the earlier its defining regime occurs, with the nearest stage corresponding to the current time.

3.3 Anisotropic percolation media

In the general case, transport in geological media is almost always anisotropic, with the anisotropy caused by factors such as the force of gravity. A description of flows in this case lies in the framework of the directed percolation problem, which was studied in Refs [52–54]. These studies show that the power-law decay of velocity correlation functions also holds in the presence of anisotropy, which, ultimately, is a consequence of the fractal medium self-similarity. However, in the presence of anisotropy, the medium properties vary differently under spatial scaling along and perpendicular to the anisotropy axis. Hence, in considering the scale invariance property of the medium, we need to introduce one more scaling index β for the coordinates in the basis plane; instead of the transformation $r \to \lambda r$, we then consider the transformation

$$\{z \to \lambda z,\ \mathbf{r}_\perp \to \lambda^\beta \mathbf{r}_\perp\}. \tag{19}$$

The analysis in [55] shows that depending on the value of β, two cases are possible: strong and weak anisotropy. For weak anisotropy $(h < 1,\ 1/(1+h) < \beta < 2/(1+h))$, transport is in a superdiffusive regime in all directions, albeit at different rates:

$$R_\parallel(t) \sim (a^h V t)^{1/(1+h)}, \qquad R_\perp(t) \sim (b^{\beta(1+h)-1} V t)^{1/[\beta(1+h)]}. \tag{20}$$

For strong anisotropy $(h < 1, \beta > 2/(1+h))$, transport is superdiffusive in the longitudinal direction as previously, but is classical diffusive in the basis plane:

$$R_\parallel(t) \sim (a^h V t)^{1/(1+h)}, \qquad R_\perp(t) \sim \sqrt{D_\perp t}. \tag{21}$$

It is important that the anisotropy is accompanied by an anomalous drift, when the mean particle displacement increases superdiffusively, just as the size of the tracer cloud along the anisotropy axis $\langle z \rangle \sim \sqrt{\langle z^2 \rangle} = R_\parallel(t)$.

We note that for anisotropic media with a finite fractality interval, there are two correlation lengths, in agreement with (19): $\xi_\parallel$ and $\xi_\perp$ related as

$$\frac{\xi_\parallel}{a_\parallel} = \left(\frac{\xi_\perp}{a_\perp}\right)^\beta, \tag{22}$$

where $a_\parallel$ and $a_\perp$ are the lower fractality bounds in the longitudinal direction and the basic plane.

On scales greater than the fractality interval, we must take the mean velocity into account, for which

$$v \approx V\left(\frac{\xi_\parallel}{a_\parallel}\right)^h . \tag{23}$$

As a result, at large times $t \gg t_\xi$, the expression for concentration takes the form

$$c \approx \frac{1}{(4\pi t)^{3/2}\sqrt{D_{\xi_\parallel} D_{\xi_\perp}^2}} \exp\left[-\frac{(z-vt)^2}{4D_{\xi_\parallel} t} - \frac{\mathbf{r}_\perp^2}{4D_{\xi_\perp} t}\right], \tag{24}$$

where

$$D_{\xi_\parallel} \sim v\xi_\parallel , \qquad D_{\xi_\perp} \sim \xi_\perp^2 t_\xi^{-1} , \tag{25}$$

and the asymptotic behavior is two-stage.

3.4 Percolation media with dual porosity

Traps are always present in real percolation media. There are at least two reasons for traps to form: first, as already mentioned, there are dead ends in the percolation cluster; second, the percolation cluster can be immersed into a porous medium of low permeability. A term describing the exchange between the backbone and traps then appears in the transport equation for quantities averaged over an ensemble of realizations, just as in the Dykhne model, in the integro-differential form

$$Q(r,t) = \frac{\partial}{\partial t}\int_0^t \varphi(t-t')\, c(r,t')\, \mathrm{d}t' , \tag{26}$$

where the integral kernel is determined by medium scale-invariance properties [56, 57]. Hence, it follows that there is a large time interval $t_1 < t < t^*$ when the kernel takes a power-law form $\varphi(t) \sim (1/t_1)(t_1/t)^\alpha$, where α characterizes the kernel decay in the self-similarity interval. At large times $t > t^*$, when traps become saturated, the kernel decays with time exponentially. As a result, the exponent characterizing the tracer cloud growth rate depends on the properties of both the velocity field and the traps [58]:

$$R(t) \sim (a^h V t_1^\alpha t)^{(1-\alpha)/(1+h)} \propto t^{(1-\alpha)/(1+h)} . \tag{27}$$

Depending on the relation between the parameters h and α (but under the condition $h < 1$), transport can be both super- and subdiffusive.

3.5 Comparison of theoretical and experimental results

To compare theoretical and experimental results, an interpolation formula relying on the results of the random advection model has been proposed, describing the behavior of concentration at a fixed distance from a tracer source as a function of time:

$$c(r,t) \propto \left(\frac{t_0}{t}\right)^{3/(1+h)} \exp\left[-\left(\frac{t_0}{t}\right)^{1/h}\right], \tag{28}$$

where t_0 and h are some tuning parameters. The experiment in [59] was carried out in fractured crystalline rock. The injection and pumping out of tracers were realized using a convergent and weakly dipole scheme. Deuterated water, bromides, and pentafluorobenzoic acid were taken as tracers for their wide range in diffusivity. The behavior of concentration turned out to be very similar for all tracers at small times and practically coincident at late times. Hence, a conclusion was drawn that the exchange of diffusive particles between a highly permeable system of cracks and a low-permeability matrix does not affect tracer transport processes. Figure 4 presents a comparison of theoretical and experimental results.

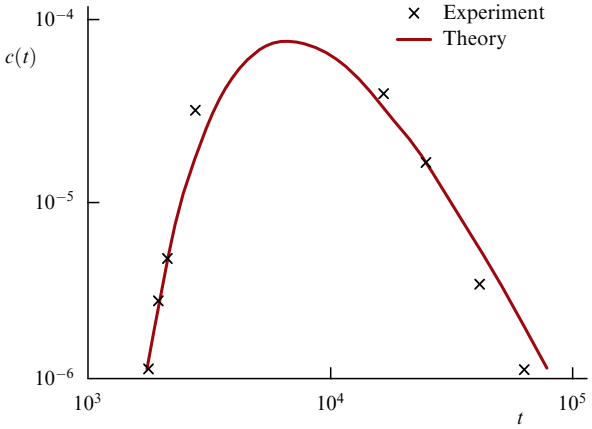

Figure 4. Comparison of computations using Eqn (28) with data from tracer experiments [59].

We note that the interpolation formula describes the experimental data well if $h \approx 0{,}4$, demonstrating that transport in the experiment occurs in a superdiffusive regime.

4. Statistically homogeneous media with dual porosity

An important (and perhaps the most frequently encountered) class of strongly heterogeneous media comprises strongly contrasting statistically homogeneous media. An example of such a medium, consisting of highly permeable channels and weakly permeable blocks filling the space between the channels, is presented in Fig. 5. It is important that nonclassical transport regimes are realized here at times when the size of the tracer cloud substantially exceeds the characteristic size of the medium heterogeneity (determined by the size of the blocks).

In the literature, the description of transport in such a medium is typically based on the Gerke–van Genuchten model [60], in which the exchange by a tracer between the fast and slow subsystems is considered in the 'mean field approximation'. This assumes that the exchange flux is

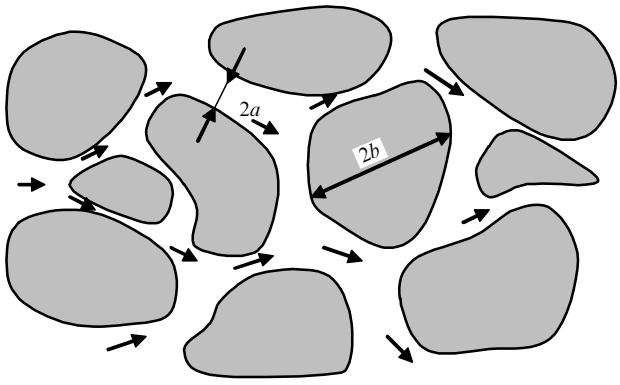

Figure 5. Diagram of a dual-porosity medium.

determined by the difference between local mean concentrations in blocks and channels. However, it can be easily shown that the time of concentration equilibration inside a weakly permeable block is very large. For example, for geological porous-fractured media, even for blocks with $b \approx 10$ cm, small on the geological scale, with a typical characteristic molecular diffusion coefficient in saturated porous media $d \approx 10^{-7}$ cm^2 s^{-1}, it would take several dozen or hundred years for the concentration to equilibrate. A proper description of transport in such time intervals therefore requires taking persistent gradients of concentration into account.

With this aim, a nonequilibrium model of dual porosity was developed in [61, 62] with the transport over long distances described by an equation for concentration in the fast subsystem (the system of channels), including a term describing the exchange between the subsystems in form (26). The expression for the kernel in Eqn (26) depends in general on the shape of weakly permeable domains, but its shape turns out to be universal [57] at small ($t \ll t_b$) and large ($t \gg t_b$) times (see below). This facilitates the description of transport regimes (including nonclassical ones) in wide time intervals.

The following results were obtained. The set of transport regimes and the order in which they follow are determined by the relation between three characteristic times t_a, t_b, and t_u. The quantity $t_a \approx a^2/d$ (an analog of the time t_1 for regular heterogeneous media), where a is the aperture of channels, describes the time when the contribution from weakly permeable regions becomes essential; $t_b \approx b^2/d$ is the time of concentration equilibration within a block; $t_u = 4d/u^2$, where u is the mean velocity of ground water filtration, characterizes the relative role of advection and diffusion in channels.

Depending on the relations between these times, there can be up to seven transport regimes. For example, in the case $t_u \ll t_a \ll t_b$, the transport is anomalous for a broad range of times $t_a \ll t \ll t_b$: the transport along the mean velocity is in the regime of quasidiffusion, when the mean displacement $\langle r_\parallel \rangle$ and the size of tracer cloud $R_\parallel$ are described by formulas (11) where $D_u = u^2 t_a$, and the transverse transport is in the regime of power-law subdiffusion described by formula (7). At small and large times, the transport is in the classical advection–diffusion regime, but with different mean velocities and effective dispersion coefficients.

5. Effects of sorption

The advantage of the approach that we have developed is that in describing nonclassical regimes, we can naturally include additional processes that have an impact on transport, for example, sorption. It is known that sorption of a tracer in a matrix in porous media leads to a substantial slowdown of the transport process. For example, at large times, the mean transport rate and the effective dispersion coefficient decrease by K times, where $K = 1 + k_\mathrm{d}$ is the so-called retardation coefficient, and the distribution coefficient k_d relates the equilibrium concentration of the tracer in a solution with the concentration of tracer adsorbed in the matrix [63]. On the other hand, if the medium contains colloidal particles (microscopic particles with a size from several dozen nanometers to several dozen micrometers, which might be present in ground waters adsorbing and carrying the tracer), this may lead to noticeable acceleration of transport in media with dual porosity. The cause of this acceleration is that

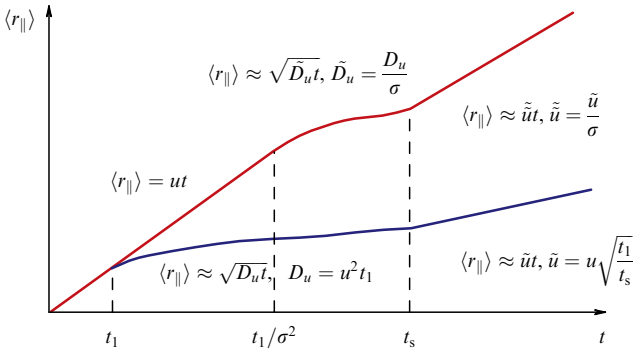

Figure 6. Mean displacement of tracer particles as they migrate in a statistically homogeneous dual-porosity medium in the presence of colloids. The time t_s corresponds to the characteristic time of the tracer concentration equilibration on the scale of porous blocks.

because of the relatively large size of colloidal particles compared to the sizes of the pores of the weakly permeable matrix, their ability to penetrate into the matrix is strongly suppressed. As a result, these particles are carried without losses at the speed of ground waters along cracks transporting the absorbed tracer.

The colloidal subsystem was taken into account in the description of tracer transport for dual-porosity media of various types in [64–66]. An important model parameter is the distribution coefficient σ linking the equilibrium values of the tracer concentration in solution c and the concentration m of the tracer absorbed on colloids,

$$c_\mathrm{eq} = \sigma m_\mathrm{eq} \,. \tag{29}$$

Figure 6 present results of computations of the mean tracer particle displacement for systems with colloids (the upper curve) and without them (the lower curve). It follows that under the condition $\sigma \ll 1$, which corresponds to the strong absorbing capacity of colloids, the presence of colloids in ground waters considerably accelerates the transport. Taking this process into account is especially important in estimating the rate of environmental pollution.

6. Transport in periodic cellular flows

The approach discussed proved convenient for building transport models in problems that seemed to have nothing in common with sharply contrasting dual-porosity media. Namely, the ideology of dual-porosity media was applied to describe transport processes in homogeneous media with regular flows [67]. It is well known that at sufficiently large Rayleigh number, periodic closed flows — chains of rolls and lattices of hexagonal cells — arise in a layer of fluid heated from below. Analyzing such flows from the standpoint of how they transport particles dissolved in fluid allows domains of two types to be singled out: those that carry tracers fast, and others that are in fact traps. Accordingly, transport in such a flow is determined by the transport through fast domains and by retardation caused by traps.

We consider a chain of rolls formed in a fluid layer of thickness H. There are two systems of subdomains in a flow structure of this type. One combines peripheral flow tubes of the thickness $w \approx \sqrt{Hd/V}$, where V is the flow velocity at the periphery and d is the molecular diffusivity. The thickness w is

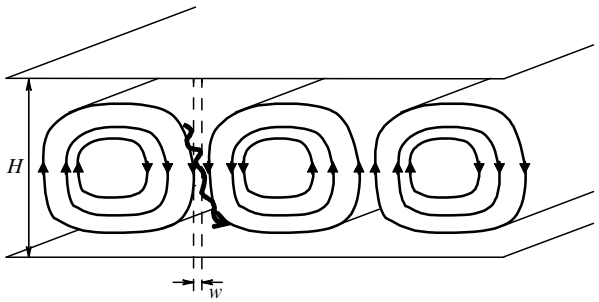

Figure 7. Schematic of the flow in a chain of rolls formed in a fluid layer heated from below.

determined from the condition that a particle moving along a separatrix between two rolls diffuses from one roll to the other. The other system is the union of roll interior regions (Fig. 7).

The first system of subdomains is analogous to the highly permeable subsystem in the dual-porosity model, whereas the interior subdomains play the role of traps. As a result, the behavior of the tracer initially concentrated, for example, at the left boundary, is described as follows. At small times $t < \tau_H$, where $\tau_H = H^2/d$ is the tracer diffusion time across the cell, transport is in a subdiffusive regime, when the growth in the cloud size in the direction of the chain is described by the expression

$$R^2 \approx 2VH\sqrt{\frac{\pi H}{V}\,t}\,. \tag{30}$$

At large times, $t > \tau_H$, the tracer propagation is described by classical diffusion with the effective coefficient [42]

$$D_{\text{eff}} \approx d\sqrt{\text{Pe}}\,, \tag{31}$$

where the Peclet number $\text{Pe} = HV/d$ is introduced for convenience.

For large Rayleigh numbers, the flow in rolls becomes fluctuating, although it keeps the form of closed cells on average (over time). In this case, the model elaborated in Ref. [67] predicts a linear increase in the effective diffusivity with an increase in the amplitude of fluctuations. This happens because in the presence of velocity fluctuations characterized by an amplitude Δv and period τ_{f}, the molecular diffusion coefficient in model expressions (for example, in Eqn (31)) has to be replaced with the effective diffusion coefficient $\tilde{d} \approx (\Delta v)^2\tau_{\text{f}}$. The conclusions from the model (the value of the diffusivity D_{eff} and its dependence on the amplitude of fluctuations) in this case are in reasonable agreement with experimental results [68].

In a periodic lattice of hexagonal cells, the flow geometry is such that active particles penetrate from one boundary tube into another at a rate that is limited by diffusion in the region close to the cell centers and not on the boundary between the cells. This is related to the widening of boundary flow tubes as they pass through the cell center. As a result, there is no increase in the effective diffusivity compared to d. But if we allow particle walk between the tubes via diffusion in the azimuthal direction, the increase in the effective diffusivity turns out to be proportional to the logarithm of the Peclet number,

$$D_{\text{eff}} \approx d\ln \text{Pe}\,. \tag{32}$$

In the range of Rayleigh numbers where the flow in the layer becomes oscillatory, the increase in D_{eff} for the lattice of hexagonal cells can be substantial. Indeed, it follows from experimental data [69] that flow fluctuations lead to intense mixing in the region close to the centers of hexagonal cells. If we introduce the mixing region size l and the characteristic mixing time τ_l, then the model in [67] predicts that the effective diffusivity is $D_{\text{eff}} \approx l^2/\tau_l$ in the case $l \ll H\,\text{Pe}^{-1/4}$, and $D_{\text{eff}} \approx H^2/(\tau_l\sqrt{\text{Pe}})$ in the opposite limit.

7. Transport processes in the presence of diffusive barriers

It was assumed in Sections 2–6 that the entire tracer is initially located directly in the migration medium. In this section, we present results for a more general problem where the tracer source is separated from the main medium by a barrier — a compact spatial region filled with a weakly permeable medium. In the presence of the barrier, the tracer is released to the main medium gradually (and varying with time), which essentially modifies transport regimes and the behavior of concentration at asymptotically large distances from the source.

In Sections 7.1–7.3, we present the problem statement and the result for a stationary barrier [70] and a barrier degrading with time [71]. For definiteness, tracer transport in the migration medium is described by the model of random advection with an infinite correlation length (see Section 3.1), and inside the barrier, by classical diffusion.

7.1 Problem statement

Because the problem is linear, the ensemble-mean tracer concentration can be written as

$$c(\mathbf{r}, t) = \int_0^t \mathrm{d}t'\, Q(t - t')\, G(\mathbf{r}, t')\,, \tag{33}$$

where $G(\mathbf{r}, t)$ is the Green's function in the prototype problem without the barrier with a given distribution of concentration at the initial moment, and $Q(t)$ is the effective tracer source rate representing the total flux of tracer particles from the barrier to the main medium. The quantity $Q(t)$ satisfies the obvious condition

$$\int_0^\infty \mathrm{d}t'\, Q(t') = N_0\,, \tag{34}$$

where N_0 is the total number of tracer particles.

The transport regimes of this problem can be conveniently characterized by the total number of active tracer particles leaving the barrier at a moment t for the migration medium,

$$N(t) = \int \mathrm{d}^3\mathbf{r}\, c(\mathbf{r}, t)\,, \tag{35}$$

and the size $R(t)$ of the main localization region

$$R^2(t) = N^{-1}(t) \int \mathrm{d}^3\mathbf{r}\, \mathbf{r}^2 c(\mathbf{r}, t)\,. \tag{36}$$

One more characteristic is the asymptotic behavior of concentration at long distances from the source:

$$c(\mathbf{r}, t) \propto \exp\bigl(-\Phi(r, t)\bigr)\,, \qquad r \gg R(t)\,. \tag{37}$$

We note that the characteristics of tracer transport in the absence of a barrier are obtained from relations (16) and (17)

if the persistent source is replaced by an instantaneous source $Q(t) \to N_0\delta(t-0)$. The size of the main localization region and the exponent in the asymptotic law for concentration for the prototype without a barrier are respectively denoted as $R_*(t)$ and $\Phi_*(r,t)$.

7.2 Stationary barrier

We assume that the barrier is a sphere filled by a weakly permeable homogeneous medium. A source initially containing N_0 tracer particles is located at the center of the sphere. Transport of a tracer within the barrier is due to classical diffusion with the coefficient d. The barrier radius R_b is small compared to all other linear sizes in the problem. The number of active particles and the size of the main localization region depend on the relation between the current time t and the characteristic diffusion time through the barrier $t_\mathrm{b} = R_\mathrm{b}^2/(4d)$. In limit cases, the quantities mentioned take the form

$$N(t) \cong N_0 \begin{cases} 4\sqrt{\dfrac{t_\mathrm{b}}{t}}\exp\left(-\dfrac{t_\mathrm{b}}{t}\right), & t \ll t_\mathrm{b}\,, \\ 1\,, & t \gg t_\mathrm{b}\,, \end{cases} \tag{38}$$

$$R(t) \sim \begin{cases} R_*\bigl(t_\mathrm{eff}(t)\bigr), & t \ll t_\mathrm{b}\,, \\ R_*(t)\,, & t \gg t_\mathrm{b}\,, \end{cases} \qquad t_\mathrm{eff}(t) = \frac{t^2}{t_\mathrm{b}}\,. \tag{39}$$

We note that the action of the barrier at small times ($t \ll t_\mathrm{b}$) not only considerably reduces the number of active particles, which becomes exponentially small, but also slows down the transport regime significantly, leading to the replacement of real time by the effective time $t_\mathrm{eff}(t) \ll t$. At large times $t \gg t_\mathrm{b}$, the influence of the barrier on the number of active particles and the transport regime ceases.

The exponent in the asymptotic law for concentration in the presence of a barrier for $t \ll t_\mathrm{b}$ is given by the expressions

$$\Phi(r,t) = \frac{t_\mathrm{b}}{t} + \frac{1}{\gamma^\gamma(1-\gamma)^{1-\gamma}}\,\frac{r}{R_*\bigl(t_\mathrm{eff}(t)\bigr)}\,, \quad \Phi_*(r,t)\frac{t}{t_\mathrm{b}} \ll 1\,, \tag{40}$$

$$\Phi(r,t) = 2\sqrt{\frac{\gamma}{1-\gamma}\,\frac{t_\mathrm{b}}{t}\Phi_*(r,t)} + \Phi_*(r,t)\,, \quad \Phi_*(r,t)\frac{t}{t_\mathrm{b}} \gg 1\,. \tag{41}$$

Hence, at small times $t \ll t_\mathrm{b}$, the asymptotic structure of concentration is two-stage. The first terms in Eqns (40) and (41) describe the number of active particles contributing to the formation of the asymptotic behavior of concentration. At large times $t \gg t_\mathrm{b}$ and at moderately long distances, when $\Phi_*(r,t)t_\mathrm{b}/t \ll 1$, the presence of a barrier does not influence the asymptotic behavior, and we have $\Phi(r,t) \approx \Phi_*(r,t)$. At even longer distances, for $\Phi_*(r,t)t_\mathrm{b}/t \gg 1$, the expression for the exponent reduces to the expression for $\Phi(r,t)$ in Eqn (41). Thus, the asymptotic behavior of concentration also remains two-stage for long times.

7.3 Degrading barrier

Of practical interest is the problem of tracer transport in the presence of a degrading barrier. In contrast to transport in the case of a stationary barrier, the tracer transport through a degrading barrier is modeled with a variable diffusion coefficient $d(t)$ that increases with time. With the dimensionless time introduces as

$$u(t) = 4R^{-2}\int_0^t d(t')\,\mathrm{d}t'\,, \tag{42}$$

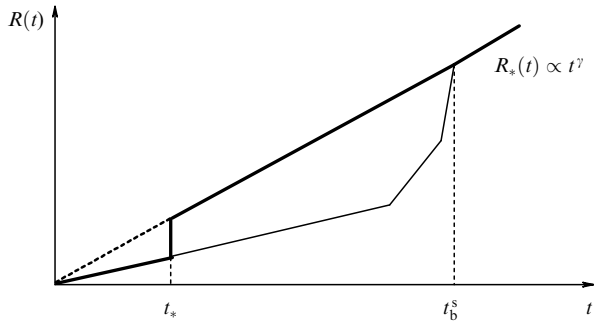

Figure 8. Size of the main localization domain (schematic) as a function of time in the case of fast degradation. The thin line corresponds to a stationary barrier, the thick line corresponds to a degrading one; t_* is the beginning of degradation, $t_\mathrm{b}^\mathrm{s} = R_\mathrm{b}^2/(4d(0))$ is the exit time from the stationary barrier.

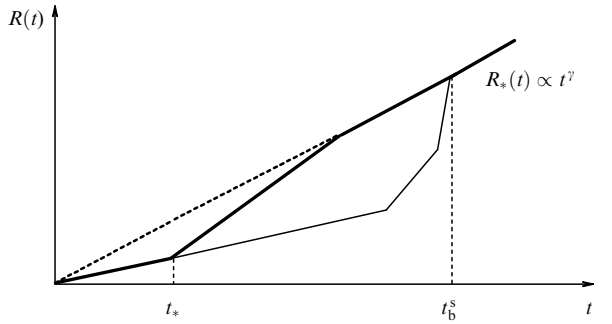

Figure 9. Size of the main localization region (schematic) as a function of time in the case of slow degradation. The thin line corresponds to a stationary barrier, the thick line corresponds to a degrading barrier; t_* is the time of the beginning of degradation, $t_\mathrm{b}^\mathrm{s} = R_\mathrm{b}^2/(4d(0))$ is the time of exit from the stationary barrier.

the results for a degrading barrier follow from formulas (39)–(42) for a stationary barrier upon the substitution

$$\frac{t}{4t_\mathrm{b}} \to u(t)\,, \quad t_\mathrm{eff}(t) \to \tilde{t}_\mathrm{eff}(t) \equiv u^2(t)\left(\frac{\mathrm{d}u}{\mathrm{d}t}\right)^{-1}. \tag{43}$$

The character of the transport regime change in real time is dependent on the degradation scenario (the dependence $d(t)$). Two limit degradation scenarios are possible: (1) A fast one, on a small time interval on which the diffusion coefficient increases practically without a bound; (2) a slow one, where the coefficient $d(t)$ increases according to a slow power law.

A schematic of the change in transport regimes with time for the fast and slow scenarios is presented in Figs 8 and 9.

8. Asymptotic approach to the description of transport processes

Commonly in the analytic description of nonclassical transport processes, the medium is assumed to be homogeneous on average, on large spatial scales. However, real media contain large-scale spatial heterogeneities. In such a situation, even classical processes of advection–diffusion require rather cumbersome numerical calculations. Additional and fundamental difficulties arise in the case of nonclassical processes, when the governing equations for concentration are integro-differential, and details of the kernels in these equation remain unknown in general.

To overcome these difficulties, a new approach based on an asymptotic description of transport processes was proposed in [72]. A practically important situation is assumed when the distance from the tracer source to the point of observation is large compared to the size of the main region of tracer localization at a given moment of time. Analysis shows that at such distances, on the one hand, the concentration formation is governed by the short-wave part of the transport mechanism, and on the other hand, the dependence of concentration on the distance to the source is exponential. Thus, formally, the situation resembles the one occurring in optics or quantum mechanics when, the geometric optics or semiclassical approximation respectively become applicable (see Refs [73, 74]). The exponent (quasieikonal) $\Gamma(\mathbf{r}, t)$, $\Gamma \gg 1$, in the expression for the concentration satisfies a first-order nonlinear partial differential equation, whose solution is sought in the framework of the canonical formalism.

As a result, we arrive at the standpoint that a concentration signal from the source reaches the observation point $\mathbf{r}$ by propagating along a linear trajectory $\{l\}$ (an analog of a ray), the form of which is found from the generalized Fermat principle

$$\delta_{\{l\},p}\left[\int_0^{\mathbf{r}} \mathrm{d}l\,\kappa(p,\mathbf{r}_l) - pt\right] = 0\,, \tag{44}$$

where $\mathrm{d}l$ is the differential element of the trajectory of the concentration signal and $\kappa(p,\mathbf{r}_l)$ is the quasi wave vector, defined by the pole nearest to the real axis in the Fourier–Laplace transform of the Green's function in the problem for a homogeneous medium with parameters coincident with those at the point $\mathbf{r}_l$ on the trajectory in a heterogeneous medium. Minimization in Eqn (44) is carried out not only over the set of concentration trajectories but also over the quasifrequency p, the Laplace variable. The coordinate origin is taken inside the region where the tracer source is localized. The quasieikonal, quasi wave vector, and quasifrequency are purely imaginary, in contrast to their real-valued analogs in geometric optics.

The tracer concentration then takes the form

$$c(\mathbf{r}, t) = A(\mathbf{r}, t)\exp\left[-\Gamma(\mathbf{r}, t)\right], \tag{45}$$

where the quasieikonal $\Gamma(\mathbf{r}, t)$ is given by

$$\Gamma(\mathbf{r}, t) = \min_{\{l\},p}\left[\int_0^{\mathbf{r}} \mathrm{d}l\,\kappa(p,\mathbf{r}_l) - pt\right], \tag{46}$$

and the pre-exponential factor $A(\mathbf{r}, t)$, being a solution of a linear partial differential equation of the first order, reduces to integrals along the concentration trajectory. The integrands are functions of medium parameters, depending on the coordinates due to the medium heterogeneity.

It is of fundamental importance that instead of determining integral kernels entering the equation for concentration, the problem solution requires only knowledge of a limited set of parameters. For example, in the random advection model, there are only three such parameters.

9. Conclusions

The main conclusions that can be drawn from the results presented in this review are as follows.

From the standpoint of nonclassical transport processes, strongly heterogeneous media can be divided into three categories: regularly heterogeneous, fractal, and sharply contrasting statistically homogeneous. In the majority of cases, a succession of transport regimes is observed with time in the main region of tracer localization. The concentration decay at distances that are asymptotically large compared to the size of the main localization region is always exponential. The change in regimes with time leads to a multistage structure of the asymptotics, with more distant stages defined by earlier transport regimes, and the nearest stage defined by the current regime.

In regularly heterogeneous media composed of a highly permeable region surrounded by a matrix of low permeability in one or two dimensions, the regimes of fast and slow classical diffusion, subdiffusion, and quasidiffusion can be realized.

The transport in isotropic fractal (percolation) media with advecting velocities characterized by sufficiently long-range correlations comes first in the superdiffusive regime, which is later replaced by classical diffusion (if the correlation length is finite).

In anisotropic fractal media with a sufficiently slow decay of spatial correlations, a superdiffusive regime is realized in the longitudinal direction, accompanied by an anomalous drift. The character of transverse transport depends on the degree of anisotropy. Superdiffusion occurs for weak anisotropy, and classical diffusion is realized for strong anisotropy.

For sharply contrasting statistically homogeneous media, there are long time intervals when the transport along the flow velocity is in the quasidiffusive regime (the mean particle displacement and the size of tracer cloud grow as the square root of time), and subdiffusion occurs in the plane perpendicular to the mean velocity.

Sorption of a tracer on colloids in sharply contrasting media can substantially accelerate the transport.

Tracer transport in a nonstationary fluid undergoing Rayleigh–Benard convection is to some degree similar to the transport in sharply contrasting media. For flows with quasi-two-dimensional cells (chains of rolls), a subdiffusive regime at small times is replaced by a diffusive regime at large times. Its effective diffusion coefficient increases by a factor of $\sqrt{\mathrm{Pe}}$ relative the molecular diffusion coefficient. For flows forming a lattice of hexagonal cells, the effective diffusion coefficient exceeds the molecular one by a factor of $\ln \mathrm{Pe}$. It can increase substantially in the presence of flow fluctuations.

The presence of a protective low-permeability barrier surrounding the tracer source leads to a substantial slowdown of transport regimes at earlier stages. The asymptotic behavior of concentration at long distances acquires an additional stage preceding the one taking place in the absence of a barrier. Barrier degradation can modify the transport regime at early times and shorten its duration.

To compute the concentration of tracers in media with large-scale heterogeneities at asymptotically large distances, a technique analogous to the semiclassical approximation (in quantum mechanics) and geometric optics can be applied. The result reduces to one-dimensional integrals along the trajectory of the concentration signal (quasi-ray), which is found based on the variational principle — an analog of Fermat's principle in geometric optics.

The authors are indebted to the Russian Science Foundation (grant no. 18-19-00533) for financial support.

References

1. Dreizin Yu A, Dykhne A M *Sov. Phys. JETP* **36** 127 (1973); *Zh. Eksp. Teor. Fiz.* **63** 242 (1973)
2. Bakunin O G *Phys. Usp.* **58** 252 (2015); *Usp. Fiz. Nauk* **185** 271 (2015)
3. Gu Q et al. *Phys. Rev. Lett.* **76** 3196 (1996)
4. Sher H, Lax M *Phys. Rev. B* **7** 4491 (1973)
5. Zelenyi L M, Milovanov A V *Phys. Usp.* **47** 749 (2004); *Usp. Fiz. Nauk* **174** 809 (2004)
6. Weiss M, Hashimoto H, Nilsson T *Biophys. J.* **84** 4043 (2003)
7. Banks D S, Fradin *Biophys. J.* **89** 2960 (2005)
8. Neuman S P *Water Resources Res.* **26** 1749 (1990)
9. Sahimi M *Phys. Rep.* **306** 213 (1998)
10. Bouchaud J-P, Georges A *Phys. Rep.* **195** 127 (1990)
11. Bolshov L, Kondratenko P, Pruess K, Semenov V *Vadose Zone J.* **7** 1135 (2008)
12. Khintchine A, Lévy P *CR Acad. Sci. Paris* **202** 374 (1936)
13. Montroll E W, Weiss G *J. Math. Phys.* **6** 167 (1965)
14. Metzler R, Klafter J *Phys. Rep.* **339** 1 (2000)
15. Sahimi M *Phys. Rev. E* **85** 016316 (2012)
16. Monin A S *Dokl. Akad. Nauk SSSR* **105** 256 (1955)
17. Balakrishnan V *Physica A* **132** 569 (1985)
18. Wyss W *J. Math. Phys.* **27** 2782 (1986)
19. Schneider W R, Wyss W *J. Math. Phys.* **30** 134 (1989)
20. Compte A *Phys. Rev. E* **53** 4191 (1966)
21. Chukbar K V *JETP* **81** 1025 (1995); *Zh. Eksp. Teor. Fiz.* **108** 1875 (1995)
22. Uchaikin V V *Phys. Usp.* **46** 821 (2003); *Usp. Fiz. Nauk* **173** 847 (2003)
23. Fisher D S *Phys. Rev. A* **30** 960 (1984)
24. Dykhne A M, Napartovich A P "Perenos rezonansnogo izlucheniya v neodnorodnoi plazme" ("Transport of resonance radiation in an inhomogeneous plasma"), Preprint (Moscow: IAE, 1970)
25. Gevorkian Z S, Lozovik Y E *J. Phys. A* **20** L659 (1987)
26. Kravtsov V E, Lerner I V, Yudson V I *Sov. Phys. JETP* **64** 336 (1986); *Zh. Eksp. Teor. Fiz.* **91** 569 (1986)
27. Deem M W *Phys. Rev. E* **51** 4319 (1995)
28. Shkilev V P *JETP* **101** 562 (2005); *Zh. Eksp. Teor. Fiz.* **128** 655 (2005)
29. Lutsko J F, Boon J P *Phys. Rev. E* **77** 051103 (2008)
30. Lutsko J F, Boon J P *Phys. Rev. E* **88** 022108 (2013)
31. Calvo I, Sánchez R *J. Phys. A* **41** 282002 (2008)
32. Klyatskin V I *Dinamika Stokhasticheskikh Sistem* (Dynamics of Stochastic Systems) (Moscow: Fizmatlit, 2002)
33. Klyatskin V I *Stokhasticheskie Uravneniya Glazami Fizika* (Stochastic Equations from a Physicist Viewpoint) (Moscow:Fizmatlit, 2001)
34. Matheron G, De Marsily G *Water Resour. Res.* **16** 901 (1980)
35. Barenblatt G I, Zheltov Iu P, Kochina I N *J. Appl. Math. Mekh.* **24** 1286 (1960); *Priklad. Mat. Mekh.* **24** 852 (1960)
36. Dykhne A M et al. *J. Hydraulic Res.* **43** 213 (2005)
37. Dvoretskaya O A, Kondratenko P S, Matveev L V *JETP* **110** 58 (2010); *Zh. Eksp. Teor. Fiz.* **137** 67 (2010)
38. Chukbar K V *JETP* **82** 719 (1996); *Zh. Eksp. Teor. Fiz.* **109** 1335 (1996)
39. Kondratenko P S, Matveev L V *JETP* **104** 445 (2007); *Zh. Eksp. Teor. Fiz.* **131** 494 (2007)
40. Dykhne A et al. *Vadose Zone J.* **7** 1145 (2008)
41. Shklovskii B I, Efros A L *Sov. Phys. Usp.* **18** 845 (1975); *Usp. Fiz. Nauk* **117** 401 (1975)
42. Isichenko M B *Rev. Mod. Phys.* **64** 961 (1992)
43. Bonnet E et al. *Rev. Geophys.* **39** 347 (2001)
44. Patashinskii A Z, Pokrovskii V L *Fluctuation Theory of Phase Transitions* (Oxford: Pergamon Press, 1979); Translated from Russian: *Fluktuatsionnaya Teoriya Fazovykh Perekhodov* (Moscow: Nauka, 1975)
45. Ma Sh *Modern Theory of Critical Phenomena* (Reading, Mass.: W.A. Benjamin, 1976); Translated into Russian: *Sovremennaya Teoriya Kriticheskikh Yavlenii* (Moscow: Mir, 1980)
46. Dykhne A M, Dranikov I L, Kondratenko P S, Matveev L V *Phys. Rev. E* **72** 061104 (2005)
47. Dranikov I L, Kondratenko P S, Matveev L V *JETP* **98** 945 (2004); *Zh. Eksp. Teor. Fiz.* **125** 1082 (2004)
48. Koch D L, Brady J F *Phys. Fluids* **31** 965 (1988)
49. Koch D L, Brady J F *Phys. Fluids* **1** 47 (1989)
50. Kondratenko P S, Matveev L V *Phys. Rev. E* **75** 051102 (2007)
51. Guyer R A *Phys. Rev. B* **34** 7816 (1986)
52. Obukhov S P *Physica A* **101** 145 (1980)
53. Cardy J L, Sugar R L *J. Phys. A* **13** L423 (1980)
54. Frey E, Täuber U C, Schwabl F *Phys. Rev. E* **49** 5058 (1994)
55. Kondratenko P S, Matveev L V *Phys. Rev. E* **83** 021106 (2011)
56. Dykhne A M, Kondratenko P S, Matveev L V *JETP Lett.* **98** 945 (2004); *Pis'ma Zh. Eksp. Teor. Fiz.* **80** 464 (2004)
57. Matveev L V *JETP* **118** 662 (2014); *Zh. Eksp. Teor. Fiz.* **145** 754 (2014)
58. Bolshov L, Kondratenko P, Matveev L, Pruess K *Vadose Zone J.* **7** 1152 (2008)
59. Becker M W, Shapiro A M *Water Resour. Res.* **36** 1677 (2000)
60. Gerke H H, van Genuchten M T *Water Resour. Res.* **29** 305 (1993)
61. Matveev L V *JETP* **115** 829 (2012); *Zh. Eksp. Teor. Fiz.* **142** 943 (2012)
62. Matveev L V *Physica A* **406** 119 (2014)
63. Rumynin V G *Geomigratsionnye Modeli v Gidrogeologii* (Geomigration Models in Hydrogeology) (St. Petersburg: Nauka, 2011)
64. Matveev L V *JETP* **108** 1044 (2009); *Zh. Eksp. Teor. Fiz.* **135** 1200 (2009)
65. Bolshov L A, Kondratenko P S, Matveev L V *Phys. Rev. E* **84** 041140 (2011)
66. Kutsepalov V A, Matveev L V *Chaos Solitons Fractals* **81** 480 (2015)
67. Matveev L V *Int. J. Heat Mass Transfer* **95** 15 (2016)
68. Solomon T H, Gollub J P *Phys. Rev.* **38** 6280 (1988)
69. Gebhart B et al. *Buoyancy-induced Flows and Transport* (Washington, D.C.: Hemisphere Publ. Corp., 1988); Translated into Russian: *Svobodnokonvektivnye Techeniya, Teplo- i Massoobmen* Vols 1, 2 (Moscow: Mir, 1991)
70. Dvoretskaya O A, Kondratenko P S *JETP* **116** 698 (2013); *Zh. Eksp. Teor. Fiz.* **143** 799 (2013)
71. Kondratenko P S, Leonov K V *JETP* **125** 340 (2017); *Zh. Eksp. Teor. Fiz.* **152** 398 (2017)
72. Kondratenko P S *JETP Lett.* **106** 604 (2017); *Pis'ma Zh. Eksp. Teor. Fiz.* **106** 581 (2017)
73. Landau L D, Lifshitz E M *Electrodynamics of Continuous Media* (Oxford: Butterworth-Heinemann, 2004); Translated from Rusian: *Elektrodinamika Sploshnykh Sred* (Moscow: Fizmatlit, 2005)
74. Landau L D, Lifshitz E M *Quantum Mechanics*: *Non-Relativistic Theory* (Oxford: Butterworth-Heinemann, 2004); Translated from Russian: *Kvantovaya Mekhanika*: *Nerelyativistskaya Teoriya* (Moscow: Fizmatlit, 2004)